Growth of $ZnS_xSe_{(1-x)}$ single crystals by CVT technique under theoretically predicted optimum condition and study of their properties

Abstract

A successful thermodynamic model for prediction of optimum temperature for the growth of binary II-VI compounds by CVT technique was extended to the ternary II-VI compounds by CVT compounds. $ZnS_xSe_{(1-x)}$ Crystals were grown in conditions predicted by this model. Structural and micro structural analyses were carried out for the grown crystals using X-ray and SEM analysis. A comparison was made between the qualities of the grown crystals for different Z values at their optimum temperature.

Introduction

ZnS and ZnS_xSe_{1-x} are important materials for the fabrication of blue or blue green light emitting device .The grown of ZnS_xSe_{1-x} has also long been of interest as the blue green emission material. Single crystals wafers of ZnS_xSe_{1-x} were used as substrates for the growth of $II-VI$ multinary epilayers. Although chemical vapor transport (CVT) can be used as an advantageous method to grow binary and ternary $II-VI$ compound single crystals at temperatures much lower than their melting points, but establishment of the optimum growth condition is always a major problem. In CVT reactor flow of the material is so much temperature dependent and control of temperature at the growth interface is always poorer than the accuracy shown by temperature controllers in the

furnace i.e. $\pm 0.1^{\circ}C$ and temperature variation up to $\pm 25^{\circ}C$ has been observed along the quartz ampoule. Good quality single crystals of this material were grown using chemical vapor transport. Using thermodynamic model and prediction of optimum condition have helped us so for to grow single crystals of binary II-VI compounds such as CdS [] and ZnS [], but this model has not been examined for ternary II-VI compounds. In This paper we have tried to extend this model to ternary compound and grow ZnS_xSe_{1-x} single crystals at theoretically predicted optimum condition. ZnS_xSe_{1-x} have been grown at predicted optimum temperatures for different x values. Structure and micromophology of the grown crystals have been studied by X-ray and SEM mesurements.

2. Experimental details

In $ZnS_xSe_{1-x} - I_2$ system at source zone, the following chemical equilibrium reaction may occur:

$$(x)ZnS + (1-x)ZnSe + I_2 \Leftrightarrow ZnI_2 + \frac{x}{2}S_2 + \frac{(1-x)}{2}Se_2 \qquad (1)$$

And at the deposition zone we have:

$$ZnI_2 + xS_2 + (1-x)Se_2 \Leftrightarrow ZnS_xSe_{(1-x)} \qquad (2)$$

It is assumed that the vapor phase contains only $ZnI_2, S_2, Se_2, I_2, and\ I$. The vapor phase chemical transport of $ZnS, ZnSe\ with\ I_2$ in a closed tube follows the individual reaction steps as given bellow:

$$ZnS + I_2 \Leftrightarrow ZnI_2 + \frac{1}{2}S_2 \tag{3}$$

$$ZnSe + I_2 \Leftrightarrow ZnI_2 + \frac{1}{2}Se_2 \tag{4}$$

$$I_2 \Leftrightarrow 2I \tag{5}$$

The equilibrium constants for reactions (3),(4) and (5) given as:

$$\begin{aligned}
\log K_3 &= 8.8 - \frac{7539}{T} + \frac{8745}{T^2} - 1.19\log T + 2.18\times10^{-6}T \\
\log K_4 &= 7.64 - \frac{5849}{T} + \frac{4154}{T^2} - 0.83\log T + 1.5\times10^{-4}T \\
\log K_5 &= 4.34 - \frac{7879}{T} + \frac{4264}{T^2} - 0.33\log T + 2.18\times10^{-5}T
\end{aligned} \tag{6}$$

The equilibrium constants for reaction (2) are given as:

$$\Delta G_1 = x\Delta G_3 + (1-x)\Delta G_4 \Rightarrow \ln K_1 = x\ln K_3 + (1-x)\ln K_4 \tag{7}$$

$$\begin{aligned}
\log K_1 &= (1.16 - \frac{1690}{T^{-1}} + \frac{12899}{T^{-2}} - 0.83\log T + 1.52\times10^{-4}T)x \\
&+ 7.64 - \frac{5849}{T^{-1}} - \frac{4154}{T^{-2}} - 0.83\log T - 1.5\times10^{-4}T
\end{aligned} \tag{8}$$

Also we can give the equilibrium constants as a function of partial pressure of the components:

$$K_{1`} = \frac{P_{ZnI_2}P_{S_2}^{x/2}P_{Se_2}^{(1-x)/2}}{P_{I_2}} \tag{9}$$

$$K_5 = \frac{P_I^2}{P_{I_2}} \tag{10}$$

And exact stochiometry of the source materials gives the following equations:

$$P_{S_2} = \frac{x}{2} P_{ZnI_2} \tag{11}$$

$$P_{Se_2} = \frac{1-x}{2} P_{ZnI_2} \tag{12}$$

Substitution of equation (11), (12) into equation (9) results:

$$P_{ZnI_2} = \left[\frac{K_1}{K_5} \left(\frac{2}{x} \right)^{x/2} \left(\frac{2}{1-x} \right)^{(1-x)/2} \right] P_I^{4/3} \tag{13}$$

The conservation of iodine gives:

$$P_{I_2}^{\circ} = P_{I_2} + \frac{1}{2} P_I + P_{ZnI_2} \tag{14}$$

Therefore we can calculate the partial pressure of different components inside the $ZnS_xSe_{1-x} - I_2$ system as a function of temperature (T) and the initial concentration of iodine (C) by numerically solving the equations (9) up to (13) for the range $700 - 1025\ C$ in $50^{\circ}C$ steps with transporter concentration of $0.5 - 15 mg/cm^3$. We can calculate $\alpha = \frac{P_{ZnI_2}}{P_{I_2}^0}$ which correlate the ratio between the number of the ZnI_2 molecules and iodine molecules inside the $ZnS_xSe_{1-x} - I_2$ system and also the difference between the α values i.e. $\Delta\alpha = \alpha(T_2) - \alpha(T_1)$. Without considering the type of migration along the tube, it can be assumed that transport rate is proportional to $\Delta\alpha$. Fig1. Shows the variation of the $\Delta\alpha$ with temperature (T) for temperature difference between two zones

i.e. $T_2 - T_1 = 50^\circ C$, different concentration C values and $x = 0.6$ For all the curves $\Delta\alpha$ changes slowly at the temperatures near to the peak positions. This shows that for a particular amount of concentration of transporter there is an optimum growth temperature for which the change in flow of material as well as its stability at the interface of the growing crystal is minimal. Selecting growth temperatures at the points nearer to for each C values reduce the sensitivity of the transport rate to the temperature fluctuations. There are very limited reports on the growth of ZnS_xSe_{1-x} single crystals by CVT technique.

In table I a comparison has been made between theoretically predicted optimum growth temperatures and experimentally applied growth temperatures. This table shows that ZnS_xSe_{1-x} single crystals with different compositions have been grown almost in same temperature whereas in our model there is a change in predicted growth temperatures change in with x and C values. Several factors cause disagreement between applied and predicted growth temperatures. The range of pressure at which the gas inside the tube should be considered as an ideal gas and mechanisms such as diffusion, convection and laminar flow involved in transport of materials inside the tube, should be considered in prediction of optimum growth temperature.

3. Crystal growth

Mixture of ZnS and $ZnSe$ has been used for the growth of ZnS_xSe_{1-x} by iodine transport method. Ampoule with the length of 160 mm and inner diameter of 12 mm was filled with 2.5 grams of heat-treated ZnS and $ZnSe$ polycrystalline powders along with iodine at a concentration of $2mg/cm^3$ of the empty space of the ampoule. The

ampoule, cooled by ice, was evacuated to 2×10^{-6} torr and sealed off. The capsule was placed into a three-zone horizontal furnace controlled by Eurotherm controllers with the accuracy of $\pm1^{\circ}C$. A reverse temperature profile was developed across the ampoule with growth zone at a higher temperature for 12 hours to remove the sticking powders from deposition zone of the ampoule and diminish the active sites. Different growth runs were carried out for the same amount of undercooling ($\Delta T = 50^{\circ}C$), starting material and ampoule geometry but with various growth temperature. The growth temperatures were selected as optimum value for $c = 2\frac{mg}{cm^3}$ which are given in table II. Each growth run was repeated twice and carried out for 12 days. At the end of each growth process, the furnace was slowly cooled to room temperature at a cooling rate of $50\frac{^{\circ}C}{hr}$ to prevent thermal strains. The compositions of the grown crystals were determined by Atomic absorption spectroscopy (AAS) measurement. The structure and morphology of the grown crystals were studied by X-ray diffraction technique the microscopic observation of the as- grown crystal surface was carried out using SEM. The result of growth runs have been summarized in table II.

Result and discussion

The result of the growth runs have been summarized in table II. Attempts were made to grown ZnS_xSe_{1-x} crystals at theoretically predicted optimum temperature for each x value. Application of theoretical model for ternary II-VI compounds by CVT technique showed results different from these we obtained for binary II-VI compounds such as

CdS[] and ZnS[]. For binary compounds the crystals grown at theoretically predicted optimum temperatures showed better quality compared to the crystals grown at temperatures different from optimum values, where as for ZnS_xSe_{1-x} only crystals grown at optimum temperature for $c = 2\frac{mg}{cm^3}$ and $x = 0.6$ showed Fairley proper quality compared to the crystals grown at optimum temperatures for $c = 2\frac{mg}{cm^3}$, $x = 0.3$ and $x = 0.9$. Figure 4(a, b, c) showed the ZnS_xSe_{1-x} crystals grown at optimum temperatures for $x = 0.3, x = 0.6$ and $x = 0.9$ respectively. In all of the growth runs, it was observed that the surfaces of the grown crystals have been contaminated by incorporation of iodine layers. All the crystals were immersed in $Na_2S_2O_3$ for few minute and washed by pure water to remove all the iodine traces from surfaces. This treatment also revealed some of etches like patterns on the surface of the grown crystals. Fig. 4.a shows the $ZnS_{0.3}Se_{0.7}$ crystals grown at $860^\circ C$. The grown crystals showed in general incomplete faces and poor crystallographic perfection due to instability in growth condition. Aggregation of crystallites for the material grown near the ampoule tip was also observed. Fig.5 shows the formation of microsteps with irregular shapes formed between two flat faces grown under this condition. A series of kinks were also observed at the surface of the grown $ZnS_{0.3}Se_{0.7}$ crystals. The formation of these types of microstructures (Fig.6) is due to rough surface of the crystals which are grown under low stability condition Fig.6 shows also a pattern like stacking disorder which looks consist of an intimate intergrowth of cubic and hexagonal structure in spite of the X-ray diffraction studies which confirmed the cubic structure for all the grown crystals. In these stacking disorders the cubic 111

planes join the hexagonal 0001 plane and these junctions are normally observed as striations parallel of these planes. Similar disorders have been observed for ZnS crystals grown from vapour [j.chem.physics 1958]. Fig4.b shows the $ZnS_{0.6}Se_{0.4}$ crystal grown at $890^{\circ}C$. The crystal is bounded by large (111) and small (010), (100) faces. A twin plane can be observed at the tip of the grown crystal. The morphology of this crystal is much similar to the morphology of the ZnS_xSe_{1-x} grown by fujita et al [JCG 47(1979)]. Fig.7 shows the etch hillocks on the (111) face of the $ZnS_{0.6}Se_{0.4}$ crystal. These crystallographic hillocks which show the structure of the grown crystals are developed due to protection of the surface against etching [etching of crystals sangvall22] Fig.4.c shows the $ZnS_{0.9}Se_{0.1}$ crystals grown at $920^{\circ}C$. A big microstructural pattern can be observed on the surface of one the crystals. This shows that growth was promoted by screw dislocation mechanism. The irregular shapes of these layers show that there has been a big difference in supersturation along the crystal surface. It was observed that etchant could only affect on (111) face of the $ZnS_{0.9}Se_{0.1}$ but the (110) face was remained unattacked by the etchant. Fig.8 shows the etch hillocks on the (111) face and Fig.9 shows unaffected (110) face of the grown $ZnS_{0.9}Se_{0.1}$ crystals. Fig. 10 shows the surface of the $ZnS_{0.9}Se_{0.1}$ crystals on which due to etching a porous structure has been produced. The porous structure looks like the aggregation of randomly oriented needles with few hundred nanometer thicknesses.

Conclusion:

ZnS_xSe_{1-x} Crystals were grown by CVT technique using iodine as the transporting agent. Growth temperature for each x value was selected based on prediction of a thermodynamic model. Result of growth runs showed that for $x = 0.6$, ZnS_xSe_{1-x} crystals were grown with bigger size and more complete faces and in general better quality compared with the crystals grown for $x = 0.3$ and $x = 0.9$. Etching the crystals faces and microstructures developed on the surface of the grown crystals confirmed the more stability condition during growth of $ZnS_{0.6}Se_{0.4}$ crystals compared to that of the $ZnS_{0.3}Se_{0.7}$ and $ZnS_{0.9}Se_{0.1}$ crystals.

Fig.1. variation of the $\Delta\alpha$ with temperature (T) for temperature difference between two zone i.e. $T_2 - T_1 = 50^\circ C$ and different concentration of transporting agent (C).

Fig.2 optimum deposition temperature crystal growth for ZnS_xSe_{1-x}.

Table.1. A Comparison between theoretically predicted optimum growth temperature and applied growth temperatures.

Fig.1

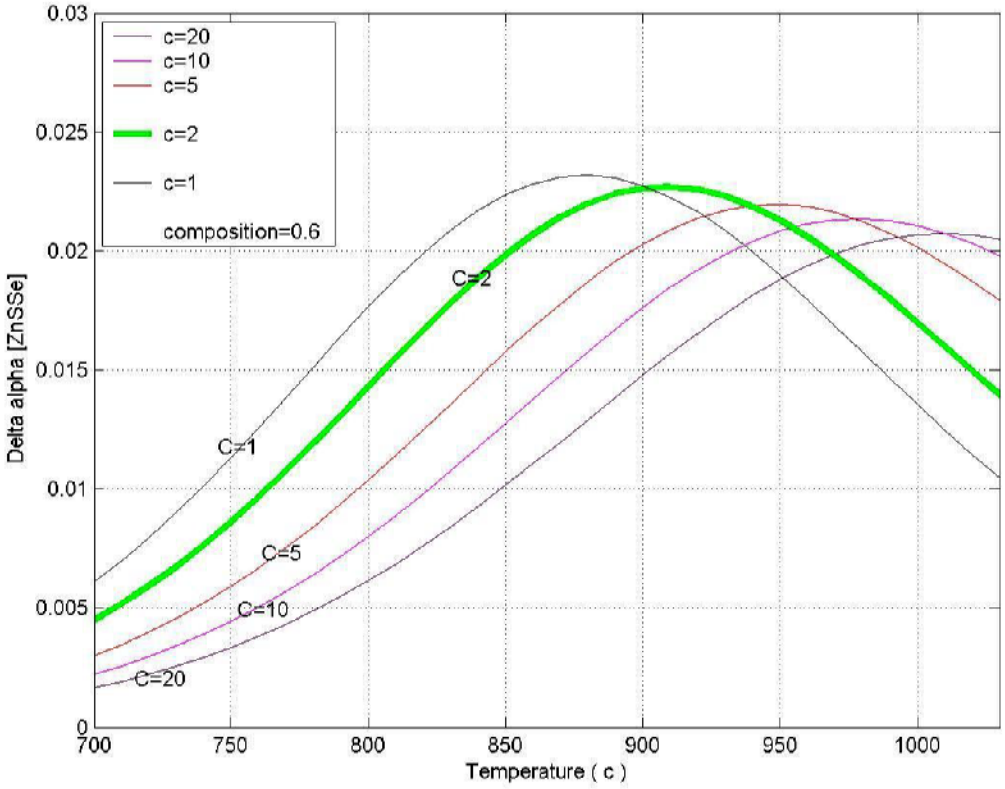
c=20
c=10
c=5
c=2
c=1
composition=0.6
C=1
C=2
C=5
C=10
C=20
Delta alpha [ZnSSe]
Temperature (c)
0.03
0.025
0.02
0.015
0.01
0.005
0
700
750
800
850
900
950
1000

Fig.2

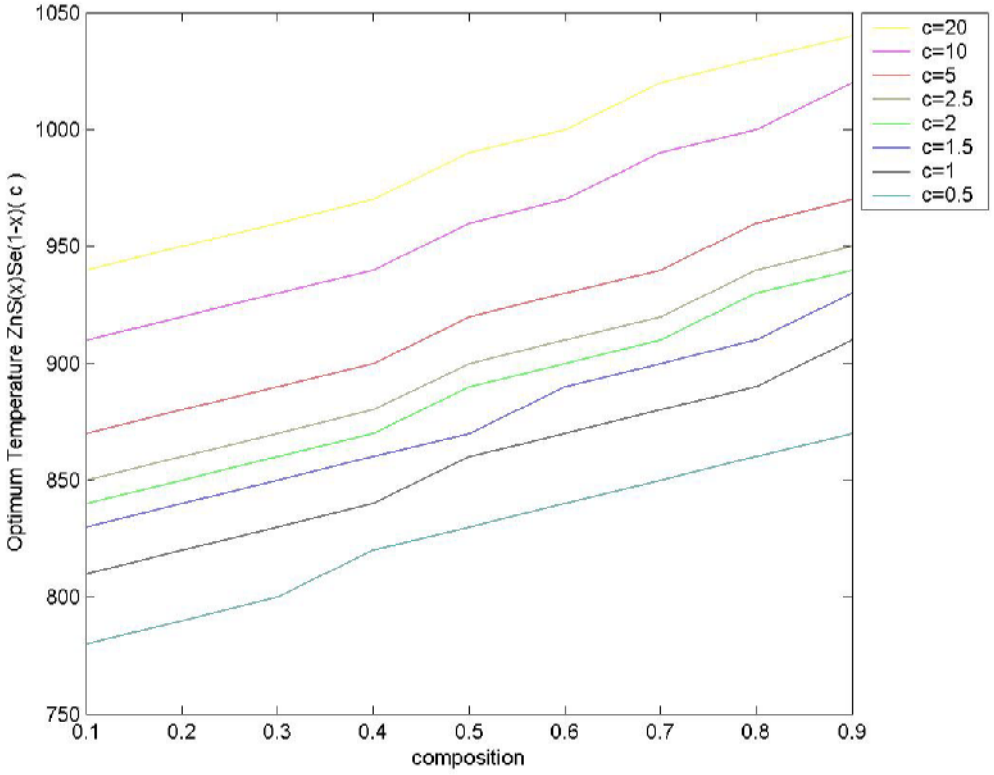
Optimum Temperature ZnS(x)Se(1-x)(c)
composition
1050
1000
950
900
850
800
750
0.1
0.2
0.3
0.4
0.5
0.6
0.7
0.8
0.9
c=20
c=10
c=5
c=2.5
c=2
c=1.5
c=1
c=0.5

Fig .3

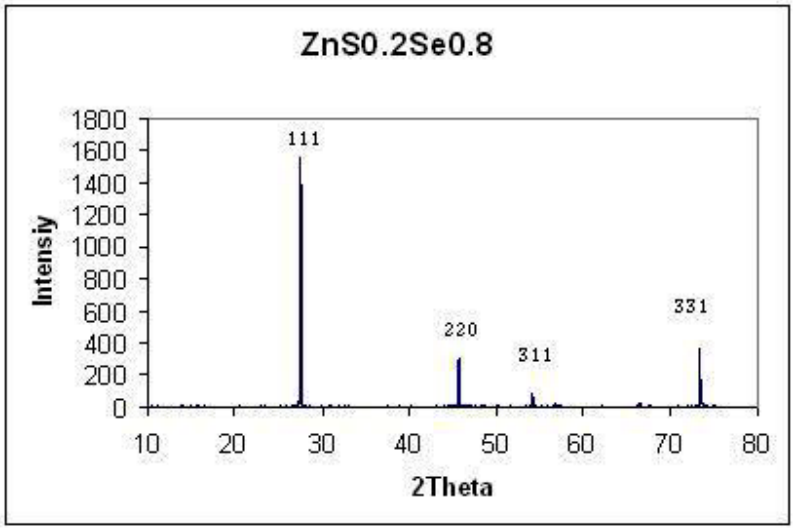
ZnS0.2Se0.8
Intensiy
1800
1600
1400
1200
1000
800
600
400
200
0
111
220
311
331
10
20
30
40
50
60
70
80
2Theta

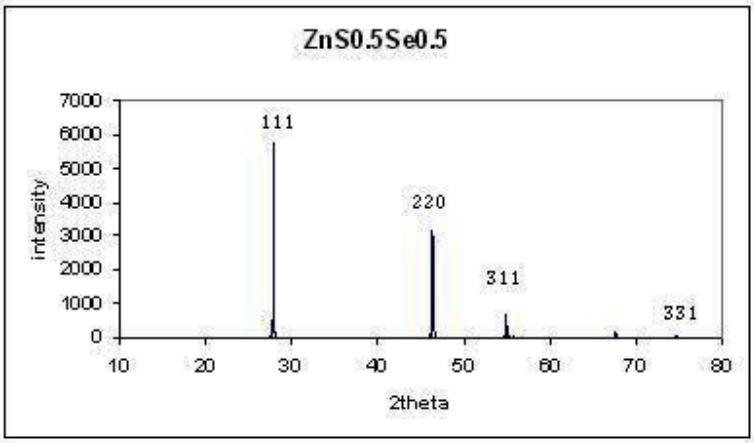
ZnS0.5Se0.5
intensity
7000
6000
5000
4000
3000
2000
1000
0
111
220
311
331
10
20
30
40
50
60
70
80
2theta

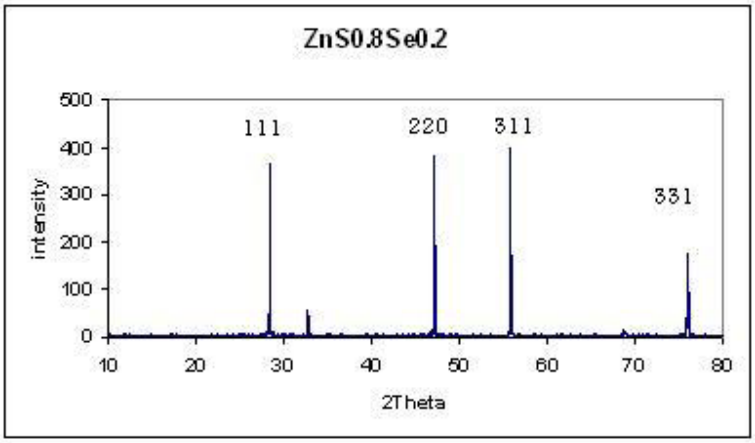
ZnS0.8Se0.2
intensity
500
400
300
200
100
0
111
220
311
331
10
20
30
40
50
60
70
80
2Theta

Fig .4.a

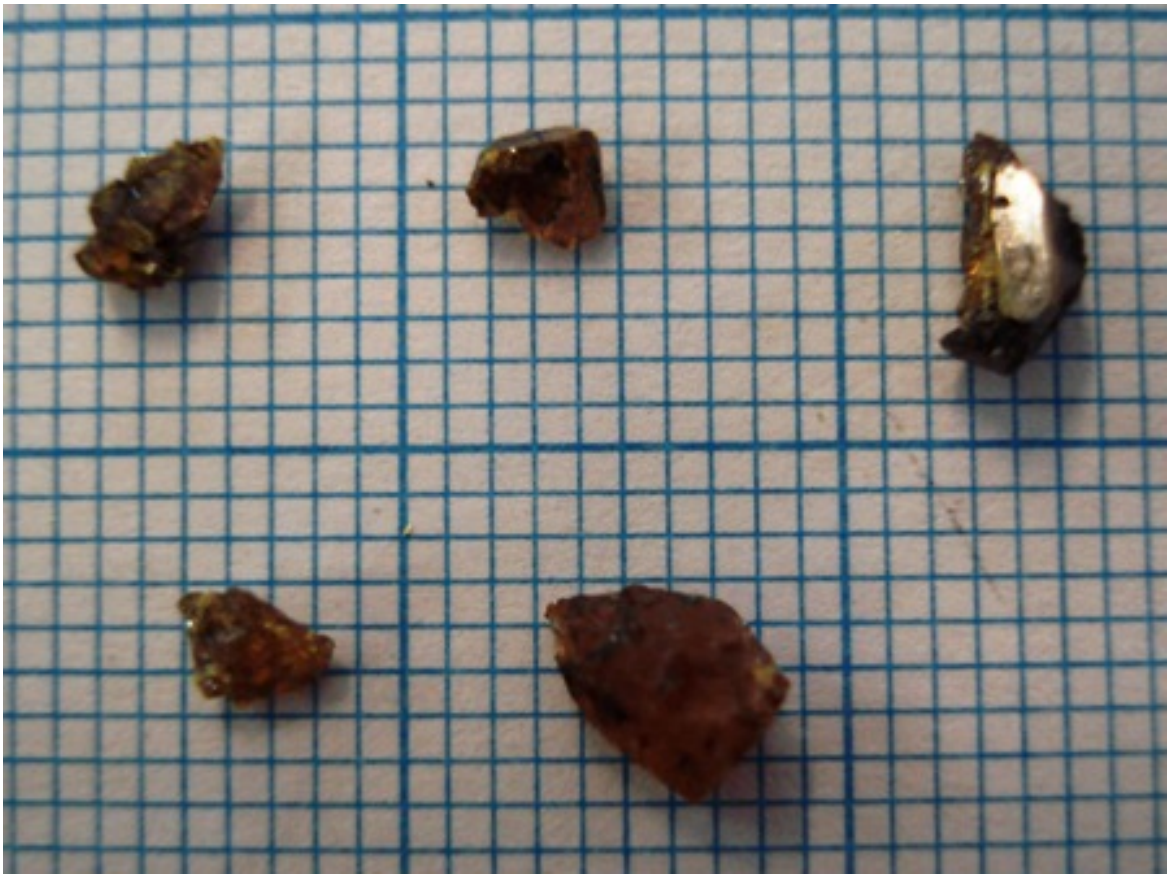

Fig 4.b

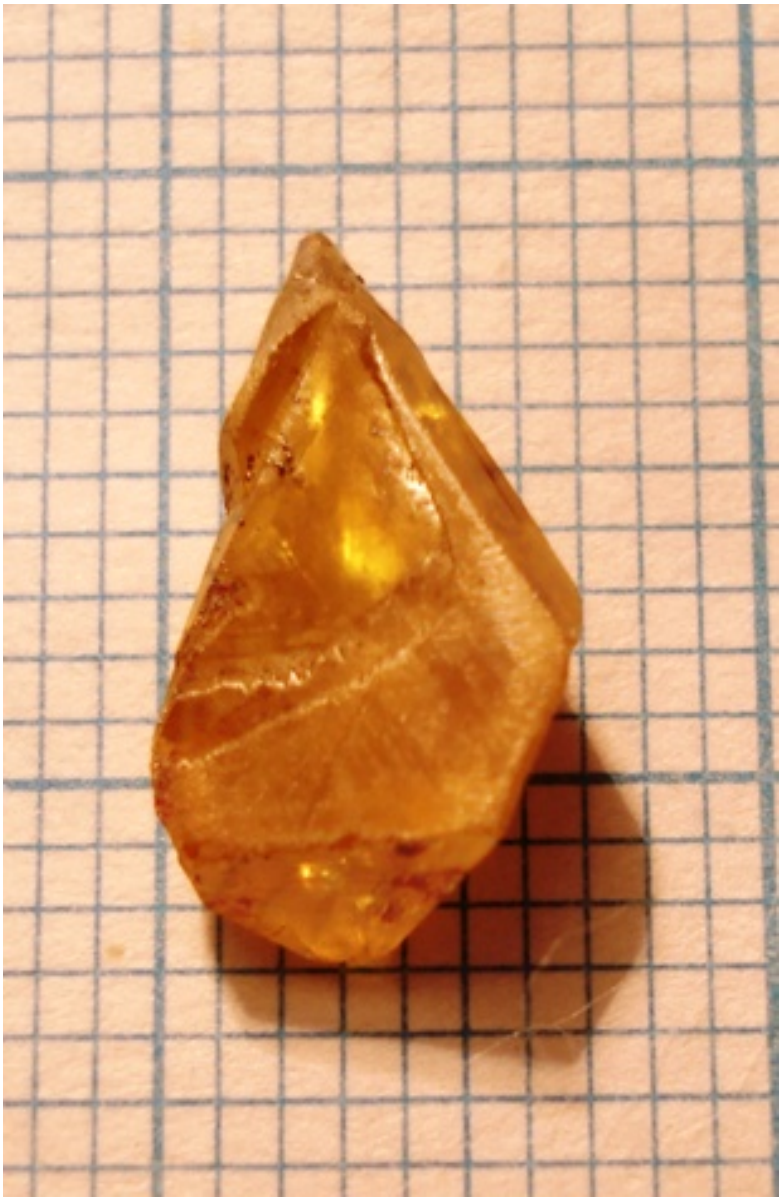

Fig 4.c

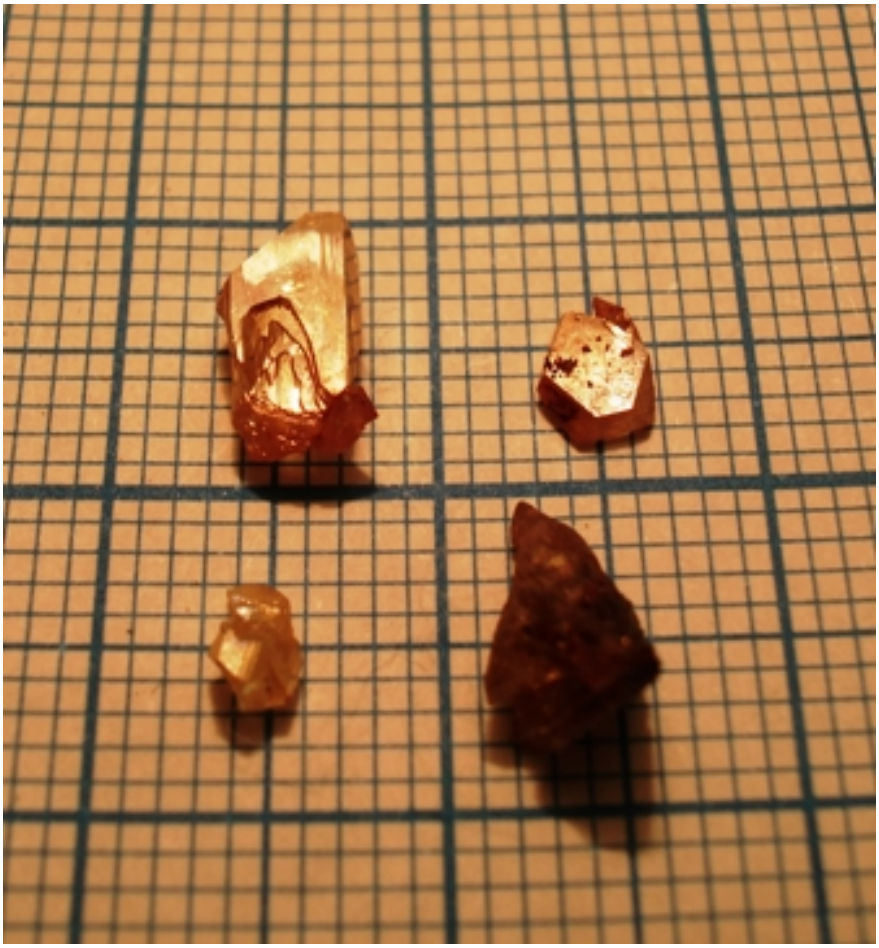

Fig 5

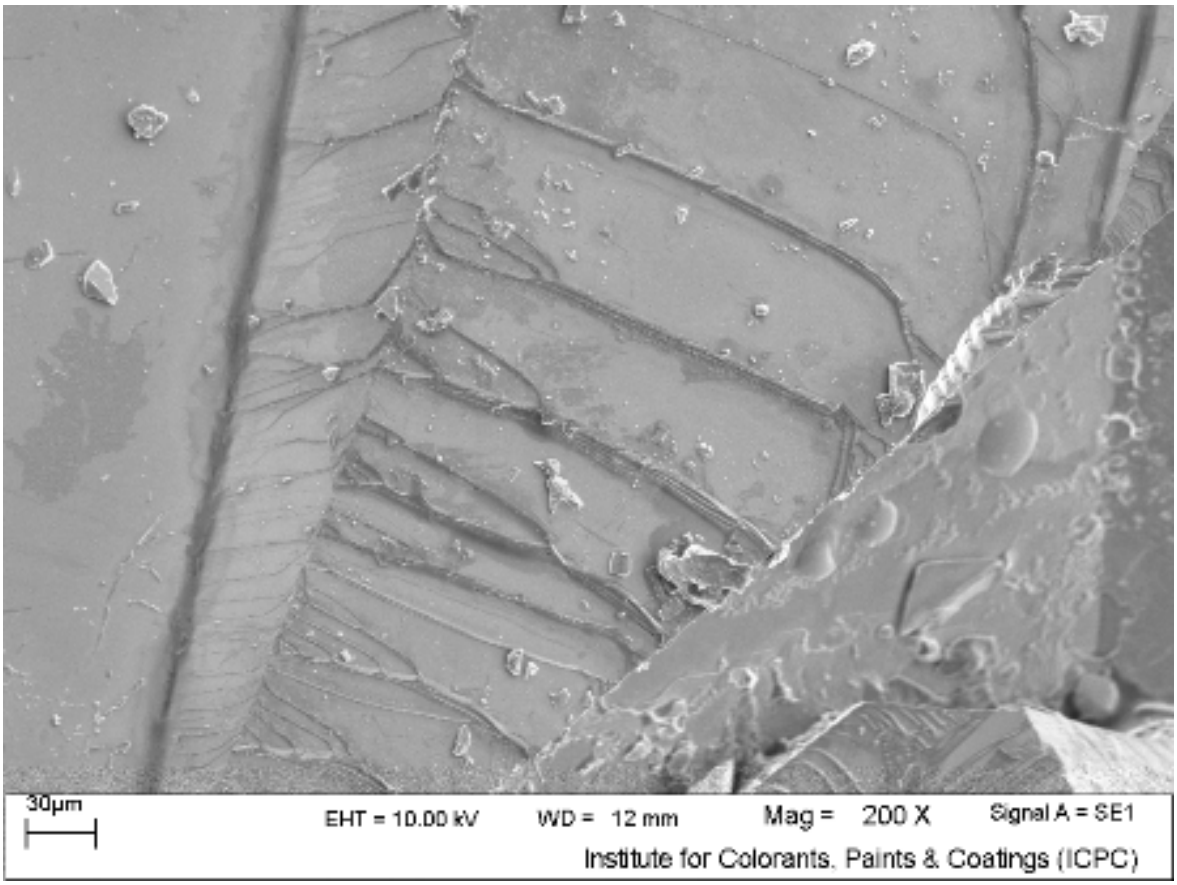
30µm
EHT = 10.00 kV
WD = 12 mm
Mag = 200 X
Signal A = SE1
Institute for Colorants, Paints & Coatings (ICPC)

Fig.6

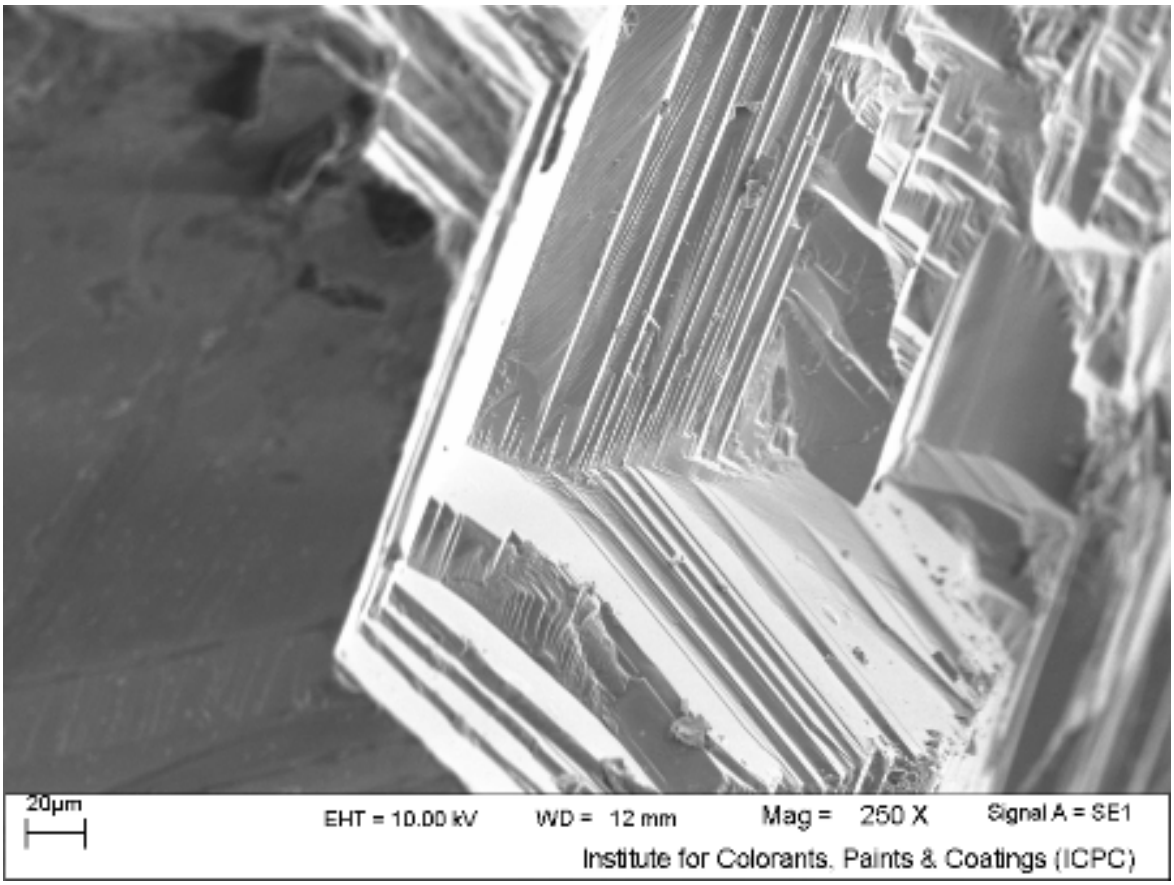
20µm
EHT = 10.00 kV
WD = 12 mm
Mag = 250 X
Signal A = SE1
Institute for Colorants, Paints & Coatings (ICPC)

Fig. 7

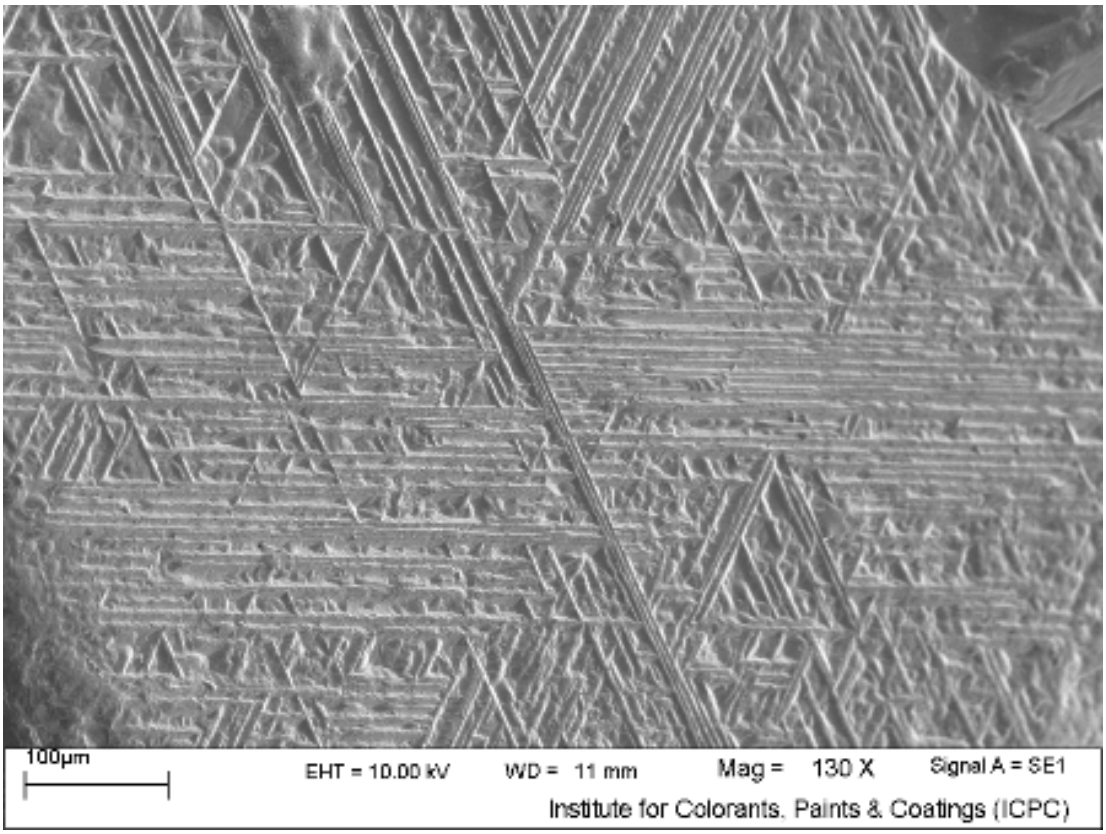
100µm
EHT = 10.00 kV
WD = 11 mm
Mag = 130 X
Signal A = SE1
Institute for Colorants, Paints & Coatings (ICPC)

Fig . 8

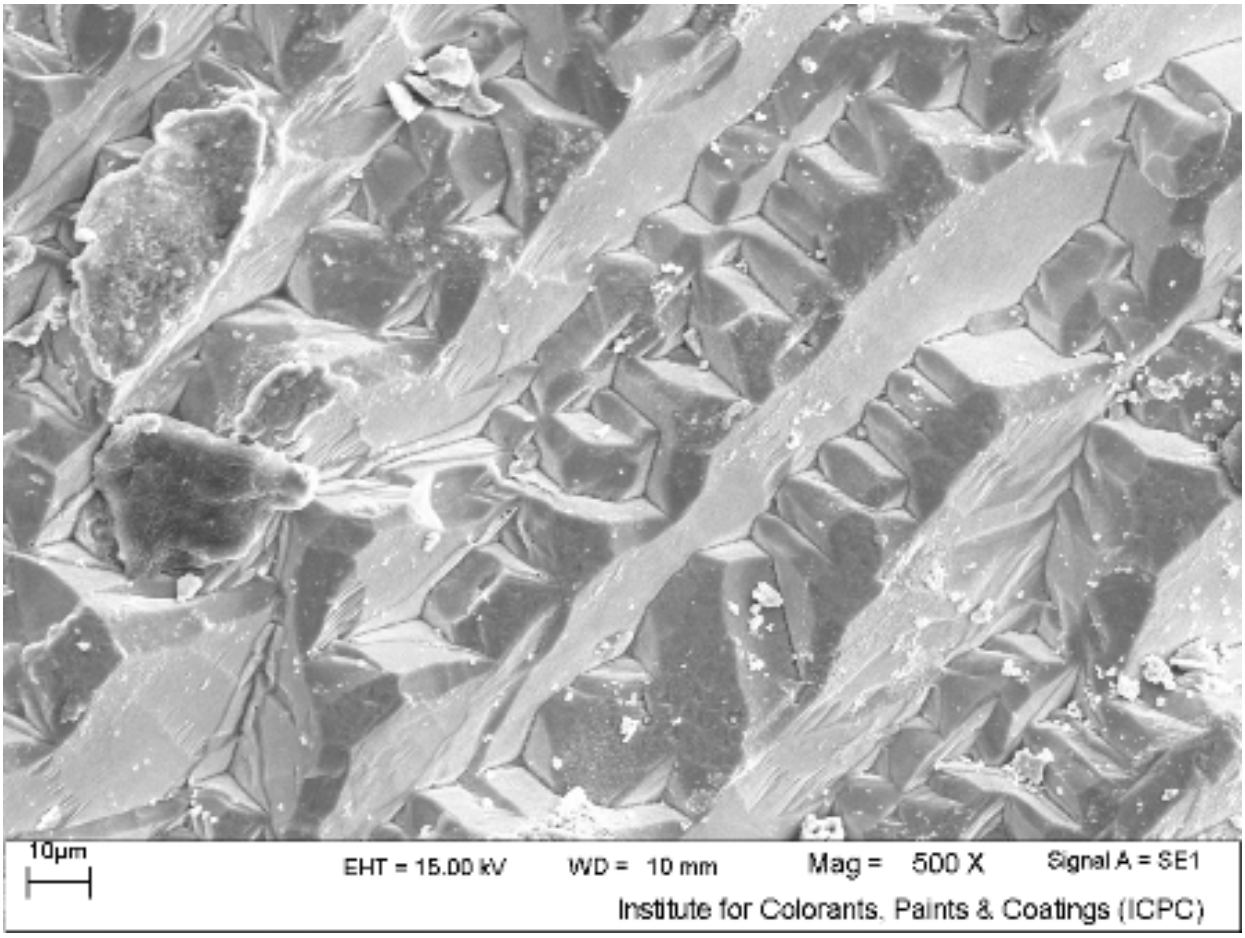
10µm
EHT = 15.00 kV
WD = 10 mm
Mag = 500 X
Signal A = SE1
Institute for Colorants, Paints & Coatings (ICPC)

Fig . 9

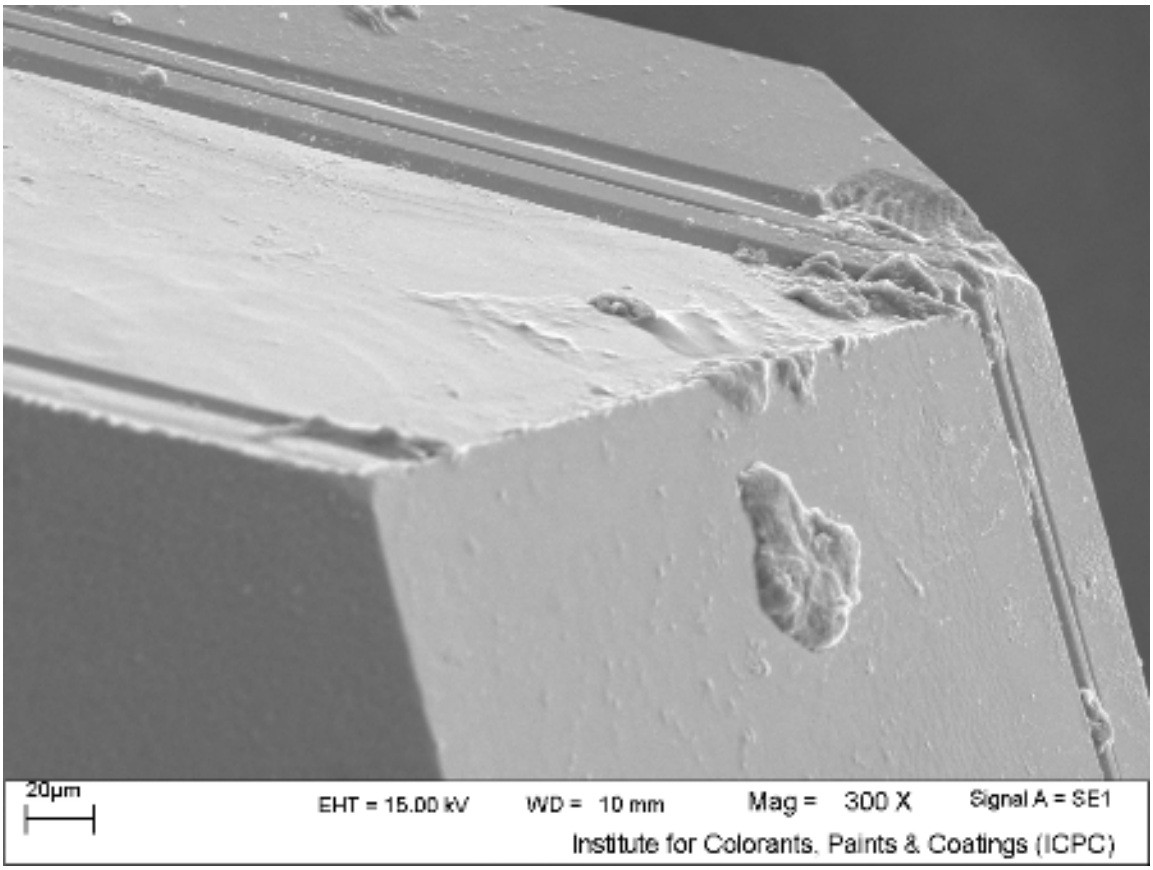
20µm
EHT = 15.00 kV
WD = 10 mm
Mag = 300 X
Signal A = SE1
Institute for Colorants, Paints & Coatings (ICPC)

Fig. 10

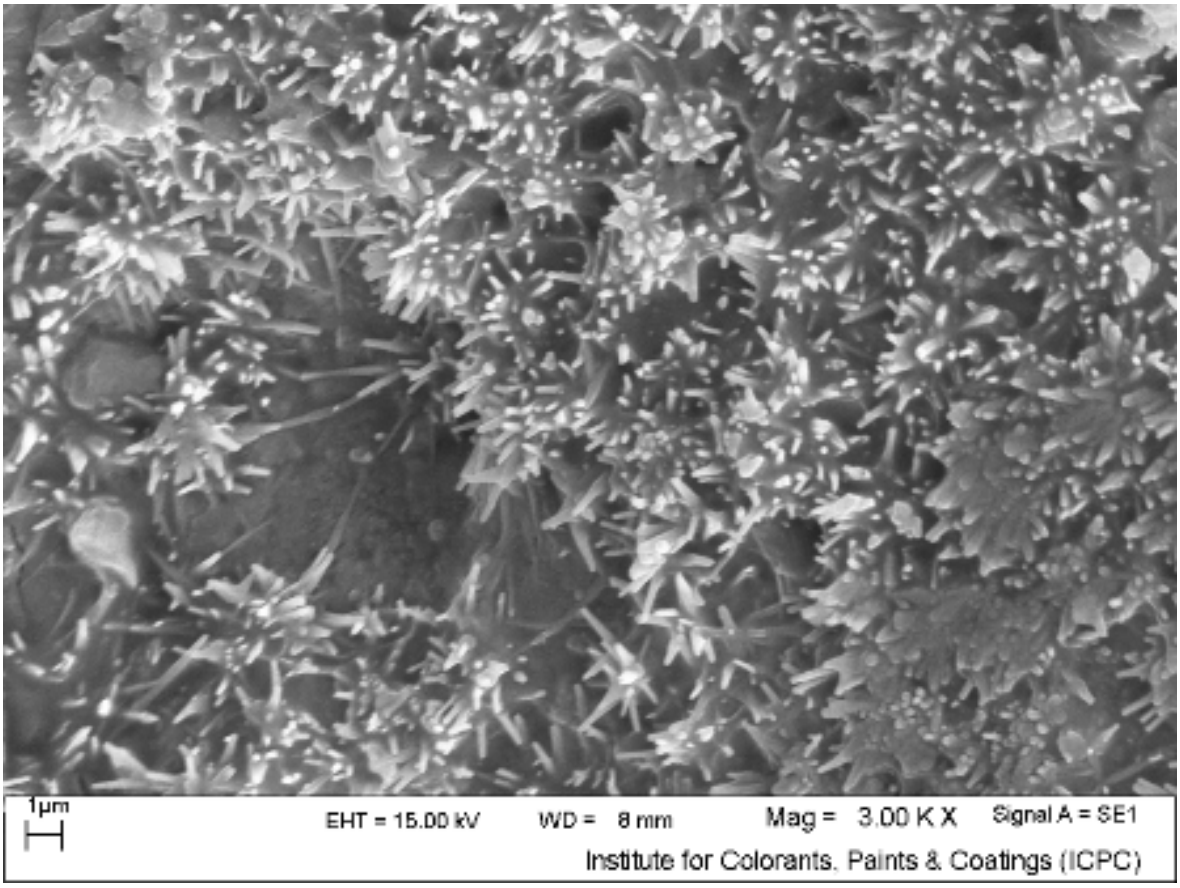
1µm
EHT = 15.00 kV
WD = 8 mm
Mag = 3.00 K X
Signal A = SE1
Institute for Colorants, Paints & Coatings (ICPC)

Table. I

Ref. No.	Growth conditions (Experimental values)				Predicted growth temperatures (^oC)	$\Delta T=T_{Exp.}-T_{Predicted}$ (^oC)
	$C\frac{mg}{cm^3}$	$T_2(^\circ C)$	$T_1(^\circ C)$	x		
[1]	5	850	840	0.2-0.8	875-910	35-60
[2]	5	850	840	0-1	875-910	35-60
[3]	2	900	860	0.4-0.6	870-900	10-40

Table. II

x	Growth parameters			Crystal habit, shape and dimensions (mm^3) (Shown in tablets)	Observed microstructures (shown in)
	C mg/cm^3	ΔT (^oC)	T_1 (^oC)		
0.30	2	50	860	Cubic, and polytypes, platelets, Tablets, prism and crystallites(Fig.4a) $3\times3\times2$ to $6\times5\times4$	Microsteps (Fig.5) Kinks(Fig.6)
0.60	2	50	890	Cubic , platelets $12\times7\times4$ Fig(4b)	hillocks (Figs.7)
0.90	2	50	920	Cubic , platelets , tablets , pyramids Fig(4c) $(4\times4\times2)$ to $(10\times5\times4)$	hillocks (Fig8) Unaffected face (Fig.9) Needles(Fig.10)